Using momentum flux measurements to determine the injection rate of a Urea Water Solution injector

Raúl Payri, Gabriela Bracho*, Pedro Martí-Aldaraví, Armando Moreno

CMT - Motores Térmicos, Universitat Politécnica de València, Spain

Abstract

The Selective Catalytic Reduction (SCR) systems technology allows the transformation of the Nitrous Oxide emissions present in exhaust gases into gaseous nitrogen and water. For a proper operation of the SCR, a urea-water solution (UWS) injector must dose an adequate amount of liquid into the exhaust pipe in order to avoid deposit formation and to guarantee the SCR system efficiency. This task requires the knowledge of the performance of the injector. Then, the goal of this work is to study the hydraulic performance of an UWS injector, by means of measuring the spray momentum flux in order to understand the influence of different variables as injected fluid, injection pressure, counter pressure and cooling temperature of the injector on the flow characteristics. The tested injector was cooled at three different temperatures, 60, 90 and 120 °C, the injection pressure of the UWS was set at 5, 7 and 9 bar, with counter pressures of 750, 900, 1000 and 2000 mbar for the two tested fluids, water and UWS. The measurements were carried out using an experimental facility developed at CMT-Motores Térmicos for the determination of spray momentum flux, where a piezoelectric pressure sensor was located near the nozzle exit of the injector, which measures the impact force of the spray. Additionally, the proposed methodology allowed to determine the injected mass flow, capturing the transient events of the injection, such as the opening and closing stages. Moreover,

*Corresponding author.
Email address: gbracho@mot.upv.es (Gabriela Bracho)

Preprint submitted to Flow Measurement and Instrumentation (Jun, 2021)

mass flow rate measurements of the injector were performed under the same operating conditions, determining the influence of the injection pressure, cooling temperature, counter pressure and fluid properties. Regarding the pressure, the tendency was as expected, the higher the injection pressure the higher the Momentum flux and flow rate. When the cooling temperature was increased the Momentum flux did not show a clear tendency. For the same conditions water has a higher momentum flux than the UWS due to differences in fluid properties and velocity at the nozzle exit. Additionally, the proposed methodology allowed to determine the injected mass flow, capturing the transient events of the injection, such as the opening and closing stages.

Keywords: Momentum Flux, UWS, Rate of Injection, SCR

1. Introduction

With the intention of reducing pollutant emissions and complying with existing regulations, Selective Catalytic Reduction (SCR) systems have been incorporated in the after-treatment of exhaust lines [1, 2].

The SCR configuration in current systems require a proper delivery of the Urea-Water Solution (UWS), most commonly known as AdBlue or Diesel Exhaust Fluid (DEF), to have efficient reduction reactions, demanding an accurate fluid dosing and ensuring a correct atomization and evaporation, in order to avoid wall impingement and deposit formation.

Therefore, the UWS injection process needs to be well understood and characterized for suitable injector selection during the design and also for the calibration process [3]. Until a few years ago the information regarding to light duty UWS injection systems was very limited. However, recently, several authors have devoted their research topic to characterize these systems and they have realized the necessity of determining the amount of injected mass [4], since it provides direct information of the unit dosage and because it is an essential parameter for correct initialization of Computational Fluid Dynamics (CFD) modelling [5, 6].

Yim et al [7] describe the decomposition of the injected UWS for SCR systems as follows. First the water present in the UWS evaporates, forming pure urea ($CO(NH_2)_2$) that can be in liquid or gaseous state:

$$NH_2{-}CO{-}NH_2(\text{aqueous}) \longrightarrow NH_2{-}CO{-}NH_2(l\,\text{or}\,\text{g}) + x\,H_2O\,(\text{gas}) \tag{1}$$

Then the thermolysis of the urea produces ammonia and isocyanic acid (HNCO):

$$NH_2{-}CO{-}NH_2(l\,\text{or}\,\text{g}) \longrightarrow NH_3(\text{gas}) + HNCO\,(\text{gas}) \tag{2}$$

Once the gases are inside of the catalyst the isocyanic acid hydrolyses into ammonia and carbon dioxide:

$$HNCO\,(\text{gas}) + H_2O\,(\text{gas}) \longrightarrow NH_3(\text{gas}) + CO_2(\text{gas}) \tag{3}$$

Observing equations 1, 2 and 3, injecting incorrect amount of UWS into the exhaust line can cause improper NOx transformation or ammonia slip into the atmosphere [8, 9]. This scenario obliges to experimentally determine the UWS mass flow rate or at least the injected mass per shot. The most used methodologies for the mass flow determination are the Bosch and the Zeuch method [4, 10]. In general, the measuring principle is based on injecting the fluid into a closed volume and registering the pressure wave generated by a piezoelectric pressure sensor, which is proportional to the injection rate. Both systems are widely used for diesel and gasoline dosing applications, where injection pressures are quite high (especially in diesel it can reach 250 MPa). Additionally, the main characteristic of those devices is that the injection is performed into a chamber filled with liquid.

However, the direct implementation of those methodologies to UWS injectors is not so simple, since the UWS injection pressures are low in comparison with diesel or gasoline direct injection systems. Moreover, real UWS injection process is in exhaust gas conditions which are considerably different to injecting into liquid and the discharge ambient pressure is low compared to those of diesel and Gasoline Direct Injection (GDI), surrounding the atmospheric pressure.

Some authors have implemented another methodology based on the momentum flux measurement [11, 12, 13, 14] for the diesel and gasoline spray, injecting into gas and obtaining good results. The fact that this technique allows to measure the evolution of the injection event in a gaseous medium makes it attractive for the application that concerns UWS dosing systems.

Currently most estimations of the mass flow rate are determined by CFD modelling of inlet and/or outlet flow [15, 16] or by collecting the injected mass of the injector in a container and assuming uniform injection events [17].

Based on the necessity of quantifying the mass flow rate for SCR dosing systems this paper focuses on the implementation of a methodology based on the momentum flux measurements in a UWS injector. The system is tested using UWS and water, which is commonly used in experimental settings due to its easy handling, similar properties and to avoid deposit formation in lab equipment.

After the measuring system is configured and validated, the test rig will be used for understanding the effect of different parameters on the evolution of the mass flow rate and injected mass.

State of the art UWS dosing systems have a cooling system that prevents the nozzle tip and the fluid from overheating due to the high exhaust gas temperatures. The cooling temperature also affects the properties of the injected fluid, even allowing it to reach flash boiling conditions if the cooling fluid is hot enough [18, 19]. The influence on the viscosity and density of the fluid can affect the hydraulic performance of the injector, therefore three cooling temperatures of 60, 90 and 120 °C have been tested.

The discharge pressure in the exhaust manifold, especially in real driving conditions, can vary depending on the engine regime and the current height above mean sea level [20, 21]. Hence the chamber pressure is set between 0.75 bar and 2 bar to quantify the effect of discharge pressure on the injector performance, which is known to affect the rate of injection and momentum flux of sprays for

Diesel and GDI injectors [14, 22, 23, 24].

A sweep of injection pressures of 5, 7 and 9 bar is also performed this is a well known effect [3, 17, 25] and will be used to corroborate the obtained results

Finally, the injected mass was also measured using a calibrated precision scale to apply the aforementioned method. The results provided useful information on the instantaneous mass flow behaviour and allowed the hydraulic characterization of the studied injector.

2. Background

The main objective of this paper is to validate a method to estimate the rate of injection for a UWS dosing system using momentum flux measurements. A relationship can be established from the definition of both variables:

$$\dot{m} = A{\cdot}\rho{\cdot}u \tag{4}$$

$$\dot{M} = A{\cdot}\rho{\cdot}u^2 \tag{5}$$

Where $\dot{m}$ is the rate of injection, A is the outlet area of the nozzle, ρ is the density of the fluid, u is the velocity of the flow at the nozzle exit and $\dot{M}$ is the momentum flux of the spray.

Combining equations 4 and 5 the momentum flux and rate of injection can be related as:

$$\dot{m} = \sqrt{A.\rho{\cdot}\dot{M}} \tag{6}$$

The real mass flux at the hole exit is determined by the velocity profile and the fluid density [26]. The real shape of the velocity profile is experimentally hard to determine but it is possible to define an effective velocity and an effective area in a sense that these are representative of the flow, as shown in figure 1.

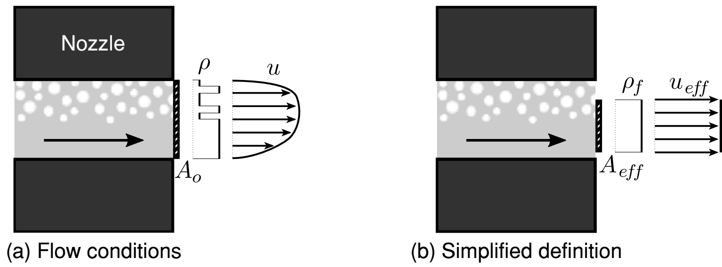

Figure 1: (a) Real Velocity profile, density and area. (b) Effective area, velocity and density in a nozzle.

The definition of these parameters is based on the consideration of a simplified flow, which is characterized by an effective area, smaller than the geometrical area, and with an effective velocity and density (equal to the fluid density) uniform in all the section. Taking this into account equations 4 and 5 can be expressed as:

$$\dot{m} = A_{eff} \cdot \rho \cdot u_{eff} \tag{7}$$

$$\dot{M} = A_{eff} \cdot \rho \cdot u_{eff}^2 \tag{8}$$

Equations 7 and 8 can be expressed in terms of the velocity u and area A by means of the discharge coefficient C_d:

$$C_d = \frac{\dot{m}}{A \cdot \rho \cdot u} \tag{9}$$

The discharge coefficient can be decomposed in two ddiferent coefficients determined C_A for the area and C_V for the velocity

$$C_d = C_A \cdot C_V \tag{10}$$

$$C_A = \frac{A_{eff}}{A} \tag{11}$$

$$C_V = \frac{u_{eff}}{u} \tag{12}$$

Based on this assumption the momentum flux and the mass flow through the hole could be defined as equation 13 and equation 14 respectively:

$$\dot{M} = C_v^2 \cdot C_A \cdot \rho \cdot A \cdot u^2 \tag{13}$$

$$\dot{m} = C_v \cdot C_A \cdot \rho \cdot A \cdot u \tag{14}$$

Combining equation 13 and equation 14 an expression for the injection rate as a function of the momentum flow is obtained as is stated in equation 15:

$$\dot{m} = \sqrt{C_A \cdot A \cdot \rho} \cdot \sqrt{\dot{M}} \tag{15}$$

Furthermore, if momentum flux can be determined experimentally, it is possible to calculate the mass flow directly from equation 15 and the injected mass from:

$$m_{inj} = \int_0^t \dot{m} \cdot dt \tag{16}$$

By measuring the injected mass, it is possible to compare the calculated injected mass with the measured one (Eq. 17) in order to obtain an adjustment coefficient K that should take a value near one if all assumptions made are correct.

$$\int_0^t \dot{m} \cdot dt = K \cdot m_{exp} \tag{17}$$

Finally, combining equations 15, 16 and 17, the mass flow can be determined as:

$$\dot{m} = K \cdot \frac{m_{exp}}{\int_o^t \sqrt{\dot{M}} \cdot dt} \cdot \sqrt{\dot{M}} \tag{18}$$

3. Methodology and Experimental Setup

Momentum flux measurements were performed on a commercial injector spray using water and urea-water solution (UWS) at a concentration of 32.5% under different discharge pressures and injector cooling temperatures. The tested injector for this study is a dossing module from Bosch, which has three orifices with a diameter of 135 µm each. During the experiments, the injector cooling temperature was set to 60, 90 and 120°C, the discharge pressure to 750, 900, 1000 and 2000 mbar and injection pressures of 5, 7 and 9 bar, in both cases referring to absolute pressure. A summary of the injector characteristics and the test conditions is provided in table 1

Table 1: Injector properties and test conditions.

Holes	3
Diameter	135 µm
Injection Pressure (absolute)	5-7-9 bar
Injector cooling temperature	60-90-120 °C
Energizing time	5 ms
Discharge Pressure (absolute)	750, 900, 1000, 2000 mbar
Fluids	Water and UWS

Using a calibrated pressure piezoelectric sensor it is possible to measure the impact force of the spray over a known surface area. The sensor is placed at a certain distance from the nozzle exit to ensure that the impingement area of the spray is within the limits of the target, as Figure 2 shows. If the sensor captures the whole spray and considering the conservation of momentum, the measured force is equal to the momentum flux at the nozzle exit [27, 28].

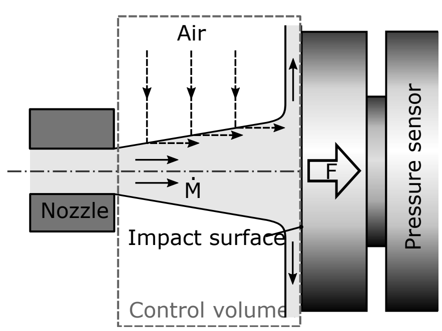

Figure 2: Momentum flux principle

The experiments were carried out in a test vessel designed to measure diesel and gasoline direct injection sprays. Originally the vessel was designed for positive back pressure levels, but due to the requirements of pressure below the atmospheric levels the test rig was adapted for working also in in vacuum pressure conditions.

To set the discharge pressure conditions a compressed air bottle was used to fill the chamber for positive counter pressures, closing the air inlet once the test conditions where reached to avoid any kind of flow from interfering with the measurements. In a similar manner, a vacuum pump was used to reach the pressures below the atmospheric conditions. Figure 3 shows a scheme of the used setup.

Some modifications to the vessel were applied to fit the tested injector. Inside the chamber, the nozzle should be aligned with the calibrated pressure piezoelectric sensor. The injector is connected to a signal generator that allows the control of the duration of the pulse which is proportional to the opening of the needle and to the duration of the injection event. A hydro-pneumatic pressurized system was used to control the injection pressure during the experiments. A cooling/heating system was connected to the injector to control the fluid temperature from 60 to 120°C

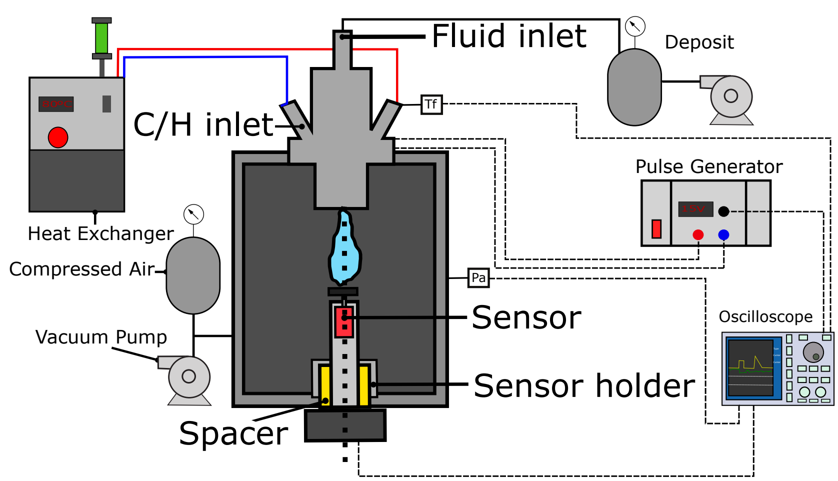

Figure 3: Experimental setup used during the Spray momentum experiments

To obtain reliable estimation of the momentum flux, fifty measurements were performed for each test condition, cleaning thoughtfully the vessel and sensor after each test to avoid deposit formation on the sensor or the nozzle.

Additionally, a scale was used to measure the injected mass using the setup in Figure 4, where 500 injections of fluid were collected. The conditions for these experiments were the same used for the momentum flux. The injected mass corresponds to the integral of the mass flow rate, therefore it will be used to adjust the curves calculated with the momentum flux measurements.

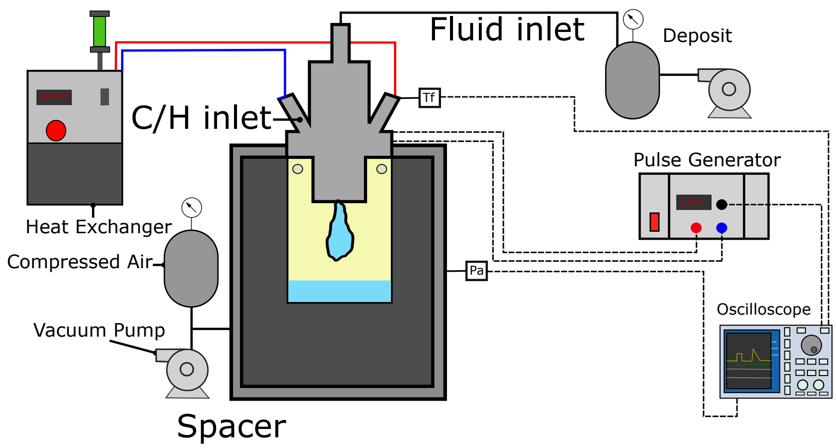

Figure 4: Experimental setup used during the experiments to collect the injected mass

The setup in Figure 4 used the same vessel that was employed in the momentum flux measurements, removing the piezoelectric sensor and replacing it with a lid. The mass was collected using a flask coupled with the injector holder. The flask has small orifices at the top that allow the pressure be the same in both the vessel and the flask. The vessel volume is big enough to keep the pressure level constant after all the injection events (difference between start and finish below 1%).

4. Results

The results of the measurements of momentum flux and injected mass under different injection pressures, ambient pressures and cooling temperatures are presented and discussed in this section. With the obtained data the Rate of Injection (ROI) of the injector is then determined. Afterwards the discharge coefficient of the nozzle is calculated for both fluids under the studied conditions.

4.1. Momentum Flux

To ensure that the distance from the nozzle to the piezoelectric sensor is enough to capture the whole impingement area and that the momentum flux average value is independent on the sensor position, different distances were tested. In figure 5 the momentum flux signals acquired for distances of 2, 5, 8 and 11 mm between the nozzle exit and the sensor are plotted.

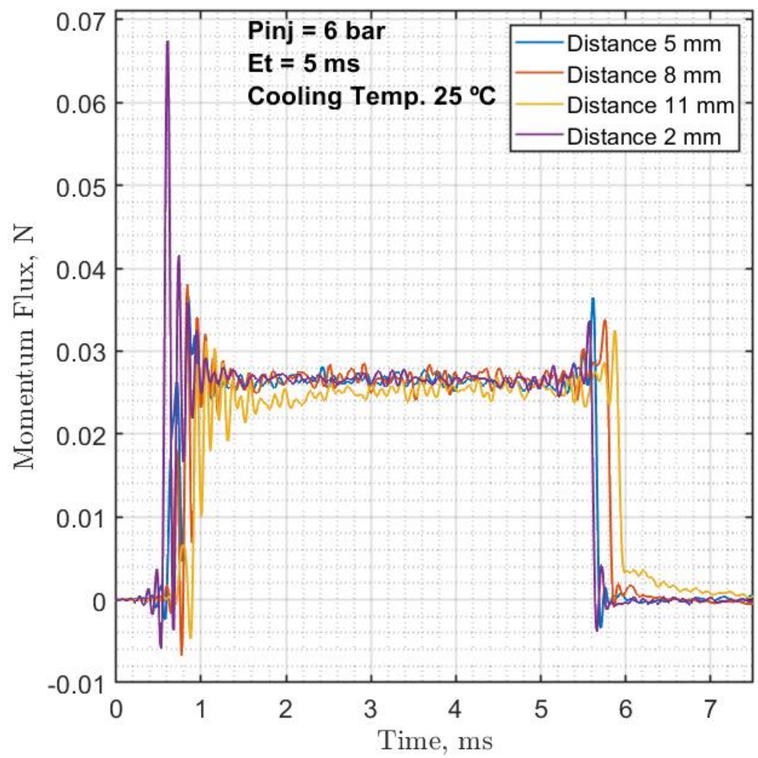

Figure 5: Momentum flux signal for different distances between nozzle and sensor

The main difference observed between signals are the starting and ending phases of the curve, where a displacement to the right due to the longer travel time (measured from the time after start of energising of the solenoid) of the spray before hitting the sensor when it is placed further away from the nozzle tip. The signals from 2, 5 and 8 mm distances are similar in the steady phase of the signal, meanwhile at 11 mm the signal is lower (on average 8% lower), which can be attributed to a cross section of the spray grater than the sensor target and thus not capturing the momentum of the whole plume.

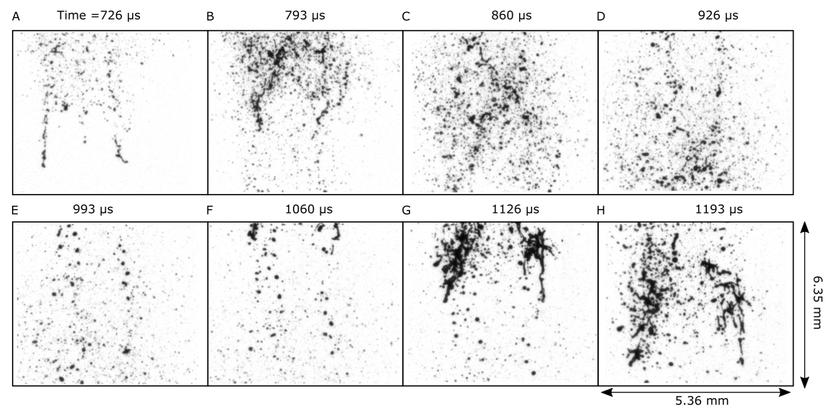

Figure 6: Spray images taken at 4 mm from the hole exit, at the initial stages of the injection event, time measured After Start Of Energising (ASOE)

Considering the results shown in Figure 5, it was decided to perform the measurements with the piezoelectric sensor at a distance of 5 mm from the nozzle exit because the stabilized signal did not differ in a significant amount respect to the signal from 2 and 8 mm. From this point forward, all the presented results correspond to the measurements of the momentum flux with the sensor at 5 mm from the nozzle exit.

The difference in the opening transient of the signals can be attributed to the packages of fluid leaving the nozzle at the beginning of the injection event, where the dynamics of the injector plays an important part. Previous visualization tests images [25] for the initial moments of the injection event are shown in figure 6, where the aforementioned packages leave the nozzle unsteadily. In the images it can be observed how droplet quantity and form vary in the first moments of the injection event, showing the initial bursts where ligaments and droplets appear increasing its density in the first four instants (A, B, C and D). Afterwards, the density of packages appears smaller for a few moments (E and F), until a new burst of packages appear showing different morphology of ligaments and bigger blobs (G and H) than those observed in the first instant.

4.1.1. *Effect of the discharge ambient pressure*

The effect of the ambient pressure and injection pressure over momentum flux is presented for water and UWS. In order to compare the effects of the different conditions over the spray momentum, an average of the steady part of the signal was calculated between the times of 2.5 ms and 5 ms after the start of energizing. Figure 7 shows a momentum flux signal over time for one of the test points and the interval where the averages are calculated is represented with red dashed vertical lines. The reason for selecting this time interval is because the signal is not affected by the transient effects evidenced at the beginning of the injection.

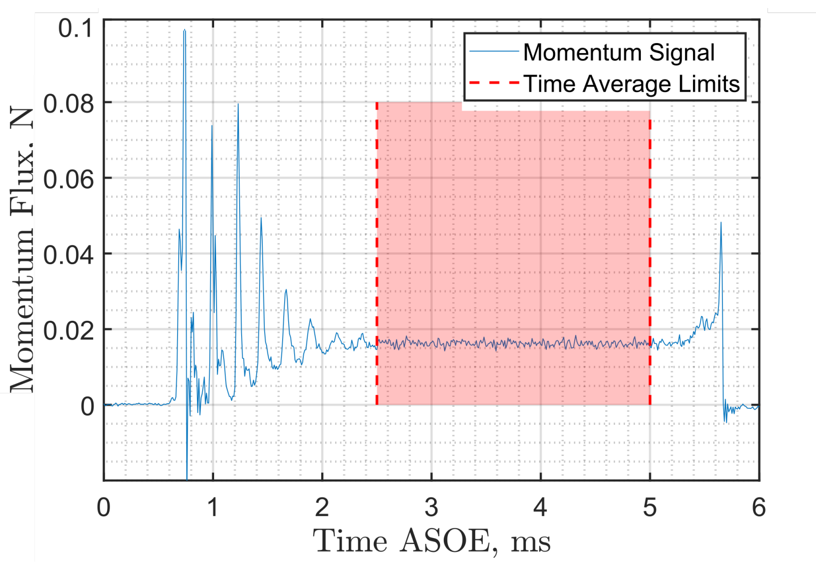

Figure 7: Momentum flux signal for an injection pressure of 5 bar at an ambient pressure of 750 mbar and a cooling temperature of 60 °C in time (ASOE)

In figure 8 it is presented the average momentum flux versus the injection pressure, where the measured average value is presented for each tested discharge pressure for both fluids.

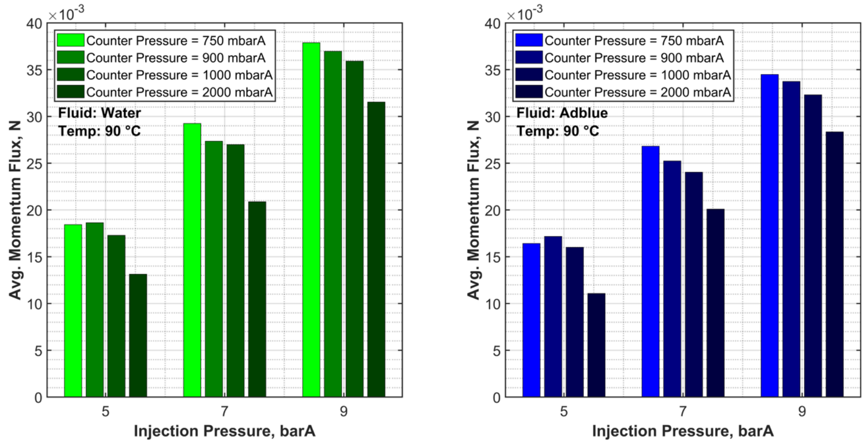

Figure 8: Effect of the discharge ambient pressure on the spray momentum flux for water (left) and UWS (right)

A trend towards lower momentum flux as the discharge pressure is increased is observed. This behaviour is logical considering equation 13, where the momentum flux depends on the square of the velocity which in turn is proportional to the square root of the pressure difference between the ambient and the inlet of the injector. This trend is observed for both fluids, water and UWS.

Since the momentum flux of the spray is proportional to the square of the mass flow, at higher altitudes (where the ambient pressure is lower) the differential pressure has to be taken into account while dosing into the exhaust stream to inject the proper amount of fluid and avoid deposit formation or urea slip.

4.1.2. Effect of the Cooling temperature

Figure 9 show the average momentum flux for the three different cooling temperatures at the three tested injection pressures. For the UWS at 5 bar it is observed a reduction of the momentum with higher cooling temperatures, meanwhile for the pressures of 7 and 9 bar there is not a clear influence of the temperature over the momentum flux.

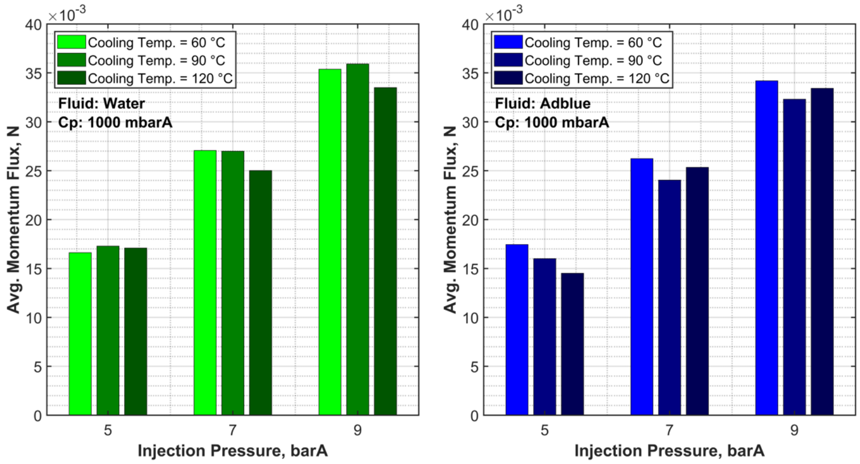

Figure 9: Effect of the cooling temperature over the spray momentum flux for Water (left) and UWS (right)

As for the water, there is a little difference at the lowest injection pressure, meanwhile as the pressure upstream is increased the effect of the cooling temperature is more evident.

Regardless of the fluid, and as reported by Brizi et al [18] for UWS and Kapusta et al [19] for water and UWS, increasing the cooling temperature and the injection pressure aids in the atomization of the spray. Furthermore, the structure of the spray changes significantly when the fluid reaches fully developed flash boiling conditions.

These authors also reported that when the flash boiling conditions are set, the spreading of the spray cone is increased, reaching lower penetration for the same pressure conditions, better atomization, enhancing evaporation and air entrainment in the spray. All these factors may have an effect on the spray momentum, possibly stopping part of the spray from hitting the target or slowing the spray and thus affecting the measurement.

4.1.3. Effect of the injected fluid

The average momentum flux for the two tested fluids with a cooling temperature of 90 °C and a counter pressure of 1 bar, for the three tested injection pressures is shown in Figure 10.

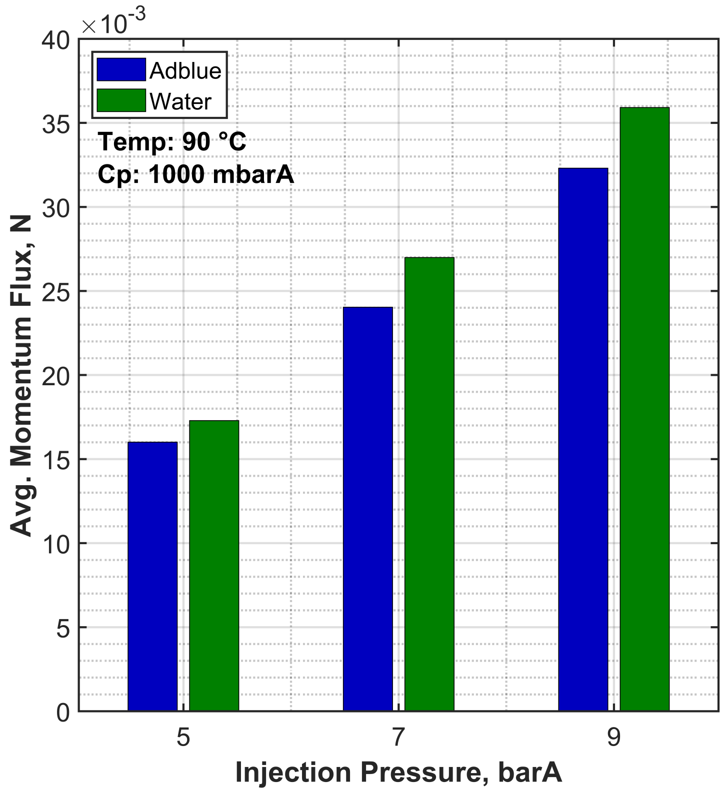

Figure 10: Effect of the injected fluid over the spray momentum flux

It is observed how the momentum flux for water is always higher than the UWS, and this results are consistent with the theory and literature. As shown in Equation 13, the spray momentum is proportional to the square of the velocity. Furthermore, Kapusta et al [17] found that for the same test conditions, the spray properties (penetration, spreading angle, unbroken liquid length) change with the injected fluid.

These results are of especial importance due to the common use of water as a substitute for UWS during experiments. This means that when water is used as a substitute for UWS some corrections should be done in terms of the momentum quantity.

Following this idea, a summary of the momentum flux averaged values is presented in Figure 11, where the momentum flux is linearly proportional to the pressure difference (ΔP)

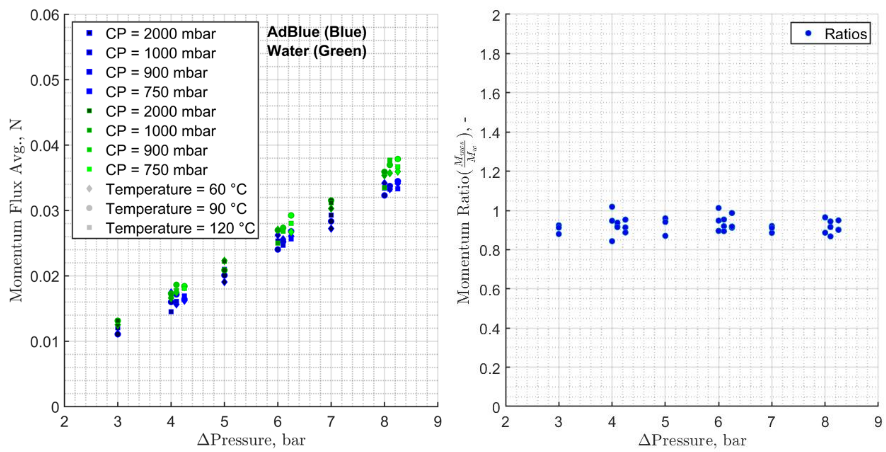

Figure 11: Average Momentum flux for all tested conditions (left) and the ratio of the average momentum flux between UWS and water (right)

In the left image a ratio R between the momentum flux of the UWS and the water is calculated for each test condition using Equation 19.

$$R = \frac{\dot{M}_{uws}}{\dot{M}_{water}} \tag{19}$$

The ratios shown in the right side of Figure 11 appear to be similar, with no clear influence of the injection pressure, cooling temperature or ambient pressure over the values. This renders possible the correction of the measurements using the ratio R when water is used as a substitute of UWS in experiments. The average ratio between all the measurements has a value of $\overline{R} = 0.924$, with an standard deviation of $s = 0.038$ or 4.17%. The ratio is related to the differences in the properties of the fluids as will be discussed later.

4.2. Injected mass

The injected mass per shot was determined by collecting the fluid of 500 shots inside of the test vessel at the test conditions and then measuring it using a scale. The design of the system ensures that most of the fluid remains inside collector, minimizing the possibility of losses due to evaporation during the measurement process. Figure 12 show the mass per shot for different fluid temperatures, injection pressure and back pressure for water (right side) and UWS (left).

It can be observed in both fluids how for similar test conditions the injected mass per shot has a similar value, noting a linear increase with the square root of the pressure difference which is in accordance with the theory.

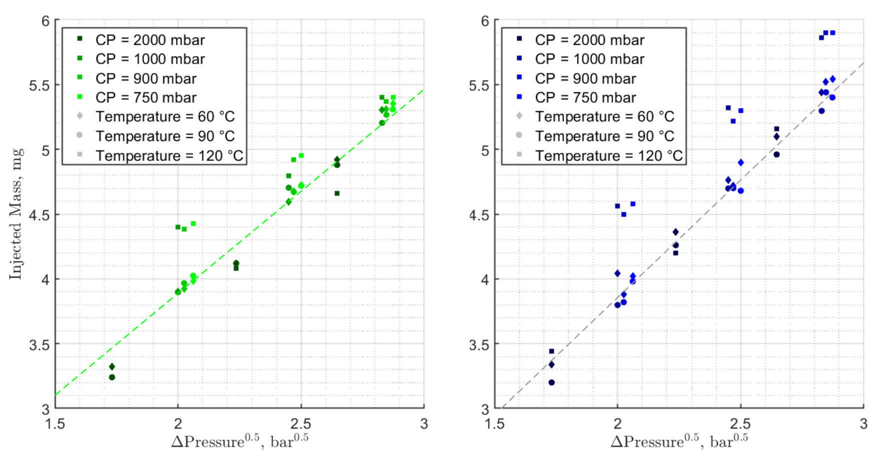

Figure 12: Injected mass for both fluids (water left, UWS right) for all tested conditions

The most remarkable aspect of the injected mass is that for the temperature of 120°C in most conditions is up to 15% higher for both fluids except for the back pressures of 2 bar, for which the measurements remain similar to other back pressures and temperatures. This behaviour could be attributed to changes in the physical properties of the fluid like the viscosity, which increases the discharge coefficient of the nozzle, together with the flash boiling conditions. To verify this hypothesis an additional investigation is proposed, using additional tools as CFD to study the internal flow at this temperatures.

Brizi [18] observed that under flash boiling conditions and after the main phase of the injection event had finished some fluid was still coming out of the injector. This effect was detected for both liquid and vapour phases under flash boiling conditions, which can explain the increase in the injected mass.

4.3. Rate of injection

With the measurements of momentum flux and injected mass, the rate of injection (ROI) curves can be calculated using the equations 16, 17 and 18. In Figure 13 the calculated rate of injection signals for a counter pressure of 1000 mbar are presented for both fluids, showing the ROI for the 3 injection pressures at each fluid temperature.

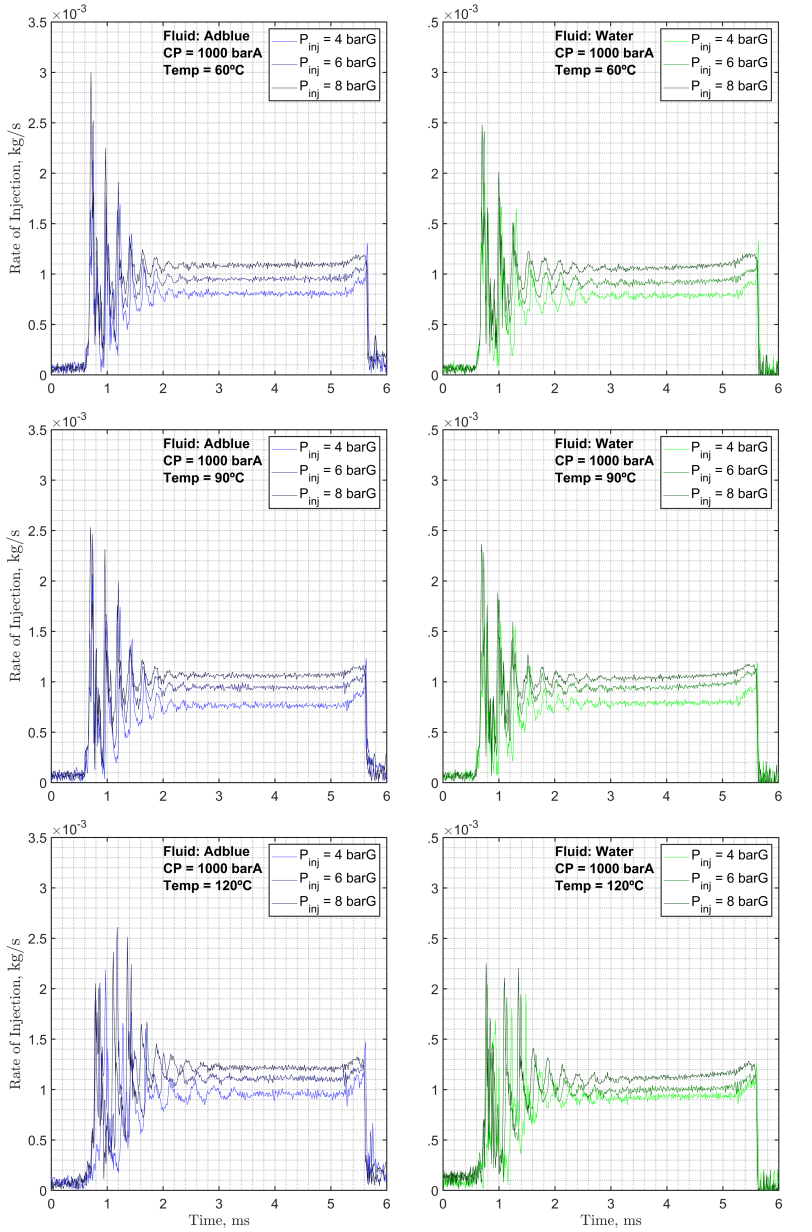

Figure 13: Calculated Rate of injection signals for different temperatures and injection pressure conditions

The most noticeable effects seen in the calculated curves are those of the injection pressure, increasing ROI for higher injection pressure levels. A similar effect is observed for the temperature, increasing the ROI as the temperature of the fluid is increased to 120°C.

Futhermore, the shape of the curves are similar for the fluid temperatures of 60°and 90°C, meanwhile for the 120°C curves a different and longer opening transient is observed. This change in the curve could indicate changes in the internal flow of the nozzle due to the change of density of the fluid or the internal dynamic behaviour of the injector.

Analogous to the momentum flux curves, an average of the ROI value was calculated using the values comprehended between 2.5 and 5 ms, where the curve is in a steady state. Figure 14 shows the average value for all the tested conditions, showing consistency with the injected mass trends.

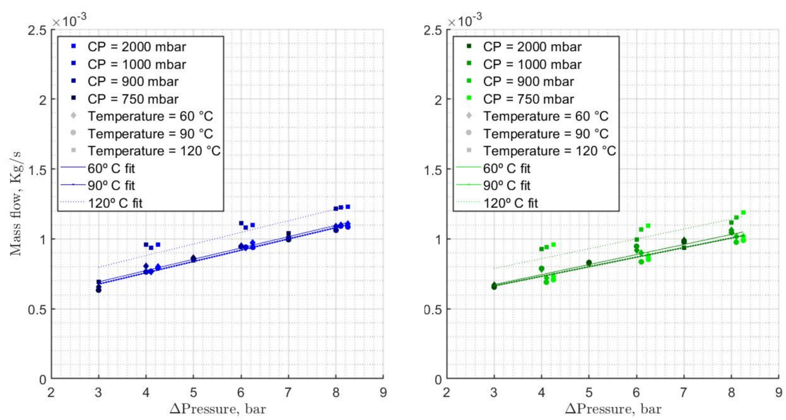

Figure 14: Rate of injection signals for different temperatures and injection pressure conditions

The ROI of injection follow a linear trend with the square root of the pressure difference. As seen before with the injected mass, when the conditions for flash boiling of the spray are set, the rate of injection is considerable higher (around 20%).

The ROI curves have been useful as an input and validation tool for current CFD models being developed [29] and it is a convenient method to characterize the injector when other known techniques are difficult or impossible to apply.

4.4. Nozzle Discharge Coefficient

Once the ROI has been calculated from the momentum flux data, it is possible to estimate the discharge coefficient of the nozzle. It is calculated by using the ROI combining Equation 9 and the Bernoulli equation for velocity $u_b = \sqrt{2\Delta P \rho_f}$ as follows:

$$C_d = \frac{\dot{m}}{A\sqrt{2\Delta P \rho_f}} \tag{20}$$

Then, the evolution of the discharge coefficient of the nozzle can be characterized in terms of the Reynolds number, which is defined as:

$$Re = \frac{\rho_f u_0 D_0}{\mu_f} \tag{21}$$

Where D_0 is the diameter of the orifice, ρ_f is the density of the fluid, u_0 the velocity at the nozzle exit and μ_f the dynamic viscosity of the fluid.

To determine the Reynolds number it is required to know the properties of the fluid at the corresponding conditions. The density used for Equations 13, 14 and 15 was calculated using the information from [30].

The viscosity of the fluid varies widely with the temperature, therefore it was calculated using an exponential decay fit with the data available in the work of Halonen et al [31]. Figure 15 shows the viscosity of water and the data points and fit used to determine this property at different temperatures for UWS.

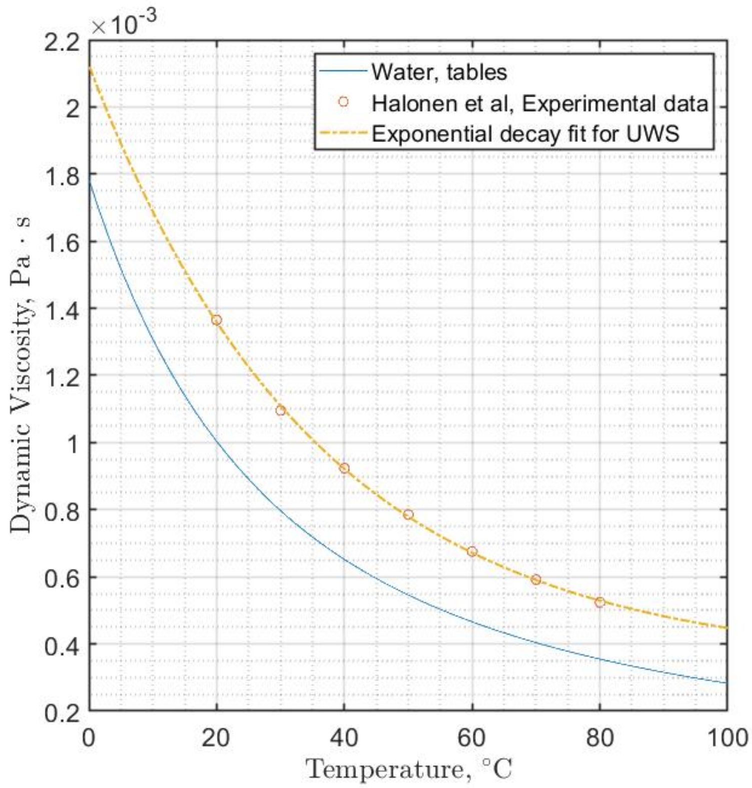

Figure 15: Viscosity of the UWS and water at different temperatures.

Figure 16 shows the discharge coefficient Cd versus the Reynolds number Re for the tested conditions, on the left image the Cd of the UWS and on the right for water.

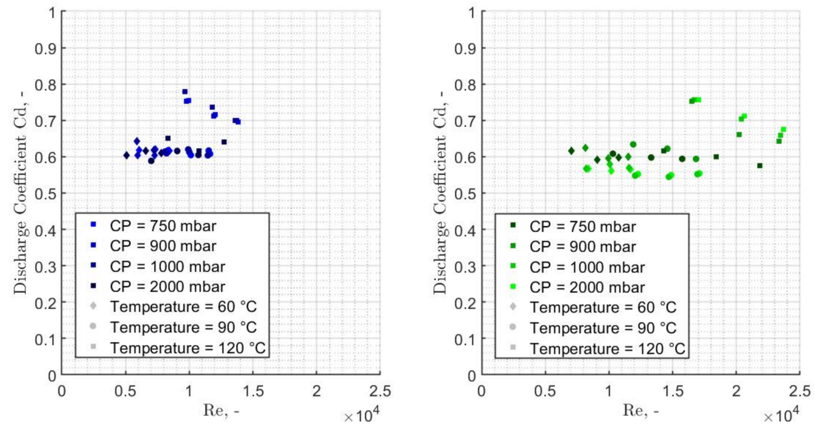

Figure 16: Discharge coefficient vs Reynolds number for each fluid at all the counter pressures and temperature of 60°C and 90°C, for UWS (left) and water (right).

In the images we can observe how the discharge coefficient of both fluids is near 0.6 for the temperatures of 60°and 90°C. Comparing the obtained value for the SCR dosing unit with other applications in engines, it is similar to the Cd of GDI injectors with a value near 0.55, but lower than diesel injectors which usually have a Cd value around 0.8 [14]. The differences can be attributed to a combination of facts. On one side, the pressures involved in the injection process of the current application is very little compared to those used in gasoline or diesel injection. On the other hand, Figure 17 shows the internal geometry of the nozzle, showing a short L/d combined with a deflection of the flow at the inlet of the orifices, which can generate some perturbations in the fluid motion.

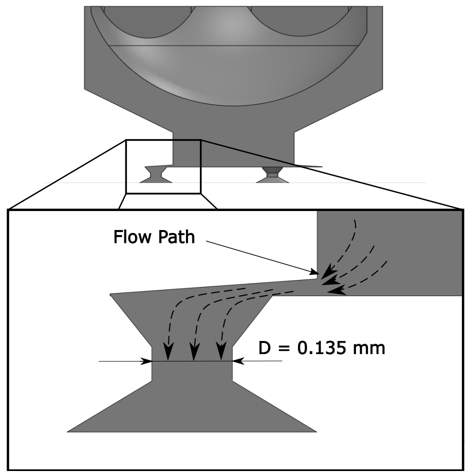

Figure 17: Section view of the internal geometry of the studied injector.

Once the fluid temperature is above the flash boiling condition and the ambient pressure is below 2 bar, a strange behavior is observed where the discharge coefficient rises nearly to 0.8 and decreasing towards 0.65 as the Reynolds number is higher (higher ΔP).

These outlier points take higher value due to the difficulty measuring its momentum flux at flash boiling conditions, where the values are considerably smaller than the values for lower temperatures at the same ΔP, resulting in higher injected mass and ROI as shown in Figures 12 and 14.

Another notable difference in Figure 16 is the higher range of Reynolds numbers for water, which can be attributed to the higher exit velocity (higher momentum flux) than for UWS and to the lower viscosity of the fluid.

5. Conclusion

A methodology to determine the rate of injection in a SCR dosing unit was employed obtaining remarking results. Normally an Injection Rate Discharge Curve indicator device based on the Bosch long tube method would be used to determine the rate of injection, but the low ΔP and the small amounts of injected mass makes hard to employ this kind of system. In this case, a methodology to measure the rate of injection using the momentum flux measurements becomes useful.

The momentum flux of the SCR system injector was measured using water and UWS as fluids. The results shows that the water has higher momentum flux than the UWS for the same testing conditions due to higher velocity of water at the exit of the nozzle.

The momentum was affected by the temperature of the fluid and the ambient pressure, showing lower momentum flux as the temperature of the spray was higher and lower momentum for higher ambient pressures.

A ratio R between the momentum flux of water and UWS was determined, finding that on average the momentum flux of UWS is 0.924 time the momentum of water.

The injected mass was also determined for all the tested conditions, increasing linearly with the square root of ΔP. Also finding that under flash boiling conditions the amount of mass injected was nearly 15% higher for both fluids. This can be attributed to the changes in the physical properties of the fluids which increases the discharge coefficient of the nozzle, combined with the effects of the flash boiling conditions.

The injected mass and momentum flux were used to determine the Rate Of Injection using Equations. 16, 17 and 18. The ROI also followed a linear behaviour with the square root of ΔP.

With the ROI, the discharge coefficients of the nozzle were calculated finding a steady value as the Reynolds number increased for most testing points, except for the points that reached flash boiling conditions.

When the flash boiling conditions for the spray are set a higher ROI and Cd were determined for both fluids. The reason behind this increase can be attributed to two factors: the internal behaviour of the nozzle and the changes in the structure of the spray (higher spreading angle) at high temperatures, leading to higher injected mass and probably not capturing the whole spray with the piezoelectric sensor (and thus leading to lower measured momentum flux).

Finally, the measuring technique is a useful tool for the hydraulic characterization of the spray, providing a valid method to accurately determine the ROI relying on the momentum flux measurements and the total injected mass. This is of importance due to the need to determine the ROI, specially when other methodologies cannot be applied, to validate CFD models and accurately dose the UWS, allowing proper reduction of emissions (NOx or Ammonia slip) and minimizing the deposit formation in the exhaust line.

6. CRediT authorship contribution statement

Raúl Payri: Supervision, Project administration, Resources, Writing - review. **Gabriela Bracho**: Supervision, Conceptualization, Methodology, Formal analysis, Investigation, Writing - Review and editing. **Pedro Martí-Aldaraví**: Writing - review and editing, Formal analysis, Investigation. **Armando Moreno**: Conceptualization, Methodology, Formal analysis, Investigation, Writing - original draft.

7. Declaration of Competing Interest

The authors declare that they have no known competing financial interests or personal relationships that could have appeared to influence the work reported in this paper.

8. Acknowledgments

This work has been partially funded by Spanish Ministerio de Ciencia, Innovación y Universidades through project RTI2018-099706-B-100.

The author A. Moreno thanks the Universitat Politècnica de València for his predoctoral contract (FPI-2018-S2-13), which is included within the framework of Programa de Apoyo para la Investigación y Desarrollo (PAID).

The Authors would like to thank Jose Enrique del Rey and Omar Huerta for their support in the experimental measurements.

References

[1] Ł. J. Kapusta, LIF/Mie Droplet Sizing of Water Sprays from SCR System Injector using Structured Illumination, Proceedings of ILASS2017 - 28th European Conference on Liquid Atomization and Spray Systems (September) (2017) 580–587. doi:10.4995/ilass2017.2017.5031. URL http://ocs.editorial.upv.es/index.php/ILASS/ILASS2017/paper/view/5031

[2] N. van Vuuren, L. Postrioti, G. Brizi, C. Ungaro, G. Buitoni, Experimental Analysis of the Urea-Water Solution Temperature Effect on the Spray Characteristics in SCR Systems, SAE Technical Paper Series 1. doi:10.4271/2015-24-2500.

[3] R. Payri, J. Gimeno, G. Bracho, A. Moreno, Spray characterization of the Urea-Water Solution (UWS) injected in a hot air stream analogous to SCR system operating conditions ., WCX SAE World Congress Experience (2019-01-0738) (2019) 1–9. doi:10.4271/2019-01-0738.Abstract.

[4] L. Postrioti, G. Caponeri, G. Buitoni, N. Van Vuuren, Experimental Assessment of a Novel Instrument for the Injection Rate Measurement of Port Fuel Injectors in Realistic Operating Conditions, SAE International Journal of Fuels and Lubricants 10 (2) (2017) 1–8. doi:10.4271/2017-01-0830.

[5] K. De Rudder, C. Chauvin, Close coupled DOC - mixer - SCR for Tier 4 final, 7th AVL International Commercial Powertrain Conference (2013) 1–10.

[6] G. Montenegro, F. Pavirani, A. Onorati, A. Della Torre, N. Rapetto, J. Campbell, E. Taffora, CFD analysis applied to the design of aqueous urea SCR dosing system with reduced risk of solid deposit formation, in: THIESEL 2018 Conference on Thermo- and Fluid Dynamic Processes in Direct Injection Engines High-pressure, 2018.

[7] S. D. Yim, S. J. Kim, J. H. Baik, I. S. Nam, Y. S. Mok, J. H. Lee, B. K. Cho, S. H. Oh, Decomposition of urea into NH3 for the SCR process, Industrial and Engineering Chemistry Research 43 (16) (2004) 4856–4863. doi:10.1021/ie034052j.

[8] R. Suarez-Bertoa, C. Astorga, Isocyanic acid and ammonia in vehicle emissions, Transportation Research Part D: Transport and Environment 49 (2016) 259–270. doi:10.1016/j.trd.2016.08.039.
URL http://dx.doi.org/10.1016/j.trd.2016.08.039

[9] J. N. Chi, H. F. M. Dacosta, Modeling and Control of a Urea-SCR Aftertreatment System Reprinted From : Diesel Exhaust Emission Control Modeling, SAE Technical Paper 2005-01-0966 114 (4) (2005) 449–464. doi:10.4271/2005-01-0966.

[10] R. Payri, F. J. Salvador, J. Gimeno, G. Bracho, A new methodology for correcting the signal cumulative phenomenon on injection rate measurements, Experimental Techniques 32 (1) (2008) 46–49. doi:10.1111/j.1747-1567.2007.00188.x.

[11] L. M. Pickett, J. Manin, R. Payri, M. Bardi, J. Gimeno, Transient Rate of Injection Effects on Spray Development, SAE Technical Paper 2013-24-0001doi:10.4271/2013-24-0001.

[12] A. Mariani, A. Cavicchi, L. Postrioti, C. Ungaro, A Methodology for the Estimation of Hole-to-Hole Injected Mass Based on Spray Momentum Flux Measurement, SAE Technical Paper Series 1. doi:10.4271/2017-01-0823.

[13] R. Payri, J. Gimeno, P. Marti-Aldaravi, D. Vaquerizo, Momentum Flux Measurements on an ECN GDi Injector, SAE Technical Paper Series 1. doi:10.4271/2015-01-1893.

[14] R. Payri, G. Bracho, J. A. Soriano, P. Fernández-Yáñez, O. Armas, Nozzle rate of injection estimation from hole to hole momentum flux data with

different fossil and renewable fuels, Fuel 279 (March) (2020) 118404. doi:10.1016/j.fuel.2020.118404.
URL https://doi.org/10.1016/j.fuel.2020.118404

[15] C. S. Kim, S. Y. Park, A design-variable-based computational study on the unsteady internal-flow characteristics of the urea-SCR injector for commercial vehicles, Defect and Diffusion Forum 379 (2017) 64–72. doi:10.4028/www.scientific.net/DDF.379.64.

[16] S. I. Lee, S. Y. Park, Numerical analysis of internal flow characteristics of urea injectors for SCR dosing system, Fuel 129 (2014) 54–60. doi:10.1016/j.fuel.2014.03.031.
URL http://dx.doi.org/10.1016/j.fuel.2014.03.031

[17] Ł. J. Kapusta, M. Sutkowski, R. Rogóż, M. Zommara, A. Teodorczyk, Characteristics of Water and Urea–Water Solution Sprays, Catalysts 9 (9) (2019) 750. doi:10.3390/catal9090750.

[18] G. Brizi, L. Postrioti, N. van Vuuren, Experimental analysis of SCR spray evolution and sizing in high-temperature and flash boiling conditions, SAE International Journal of Fuels and Lubricants 12 (2) (2019) 87–107. doi:10.4271/04-12-02-0006.

[19] Ł. J. Kapusta, R. Rogoz, J. Bachanek, Ł. Boruc, A. Teodorczyk, Low-Pressure Injection of Water and Urea-Water Solution in Flash-Boiling Conditions, in: SAE Powertrains, Fuels & Lubricants Meeting, SAE International, 2020.

[20] Y. Y. Wang, I. Haskara, Exhaust pressure estimation and its application to detection and isolation of turbocharger system faults for internal combustion engines, Journal of Dynamic Systems, Measurement and Control, Transactions of the ASME 134 (2). doi:10.1115/1.4005045.

[21] J. M. Luján, J. R. Serrano, P. Piqueras, B. Diesel, Turbine and exhaust ports thermal insulation impact on the engine efficiency and aftertreatment

inlet temperature, Applied Energy 240 (June 2018) (2019) 409–423. doi:10.1016/j.apenergy.2019.02.043.
URL https://doi.org/10.1016/j.apenergy.2019.02.043

[22] R. Payri, G. Bracho, J. Gimeno, A. Bautista, Rate of injection modelling for gasoline direct injectors, Energy Conversion and Management 166 (February) (2018) 424–432. doi:10.1016/j.enconman.2018.04.041.
URL https://doi.org/10.1016/j.enconman.2018.04.041

[23] R. Payri, J. Gimeno, C. Mata, A. Viera, Rate of injection measurements of a direct-acting piezoelectric injector for different operating temperatures, Energy Conversion and Management 154 (2018) 387–393. doi:10.1016/j.enconman.2017.11.029.
URL https://doi.org/10.1016/j.enconman.2017.11.029

[24] R. Payri, J. Gimeno, P. Martı-Aldaravi, A. Viera, Measurements of the mass allocation for multiple injection strategies using the rate of injection and momentum flux signals, International Journal of Engine Researchdoi:10.1177/1468087419894854.

[25] R. Payri, G. Bracho, J. Gimeno, A. Moreno, Investigation of the urea-water solution atomization process in engine exhaust-like conditions, Experimental Thermal and Fluid Science 108 (May) (2019) 75–84. doi:10.1016/j.expthermflusci.2019.05.019.
URL https://doi.org/10.1016/j.expthermflusci.2019.05.019

[26] R. Payri, J. M. García, F. J. Salvador, J. Gimeno, Using spray momentum flux measurements to understand the influence of diesel nozzle geometry on spray characteristics, Fuel 84 (5) (2005) 551–561. doi:10.1016/j.fuel.2004.10.009.

[27] J. Gimeno, Desarrollo y aplicación de la medida de flujo de cantidad de movimiento de un chorro Diesel, Ph.D. thesis, E.T.S. Ingenieros Industriales, Universidad Politécnica de Valencia (2008). doi:10.4995/Thesis/

10251/8306.
URL https://riunet.upv.es/handle/10251/8306

[28] J. M. Desantes, R. Payri, F. J. Salvador, J. Gimeno, Prediction of Spray Penetration by Means of Spray Momentum Flux, SAE Technical Paper 2006-01-1387doi:10.4271/2006-01-1387.

[29] R. Payri, G. Bracho, P. Mart, J. Marco-gimeno, G. Bracho, P. Mart, P. Martí-Aldaraví, J. Marco-gimeno, Computational study of urea-water solution sprays for the analysis of the injection process in SCR-like conditions, Industrial & Engineering Chemistry Researchdoi:10.1021/acs.iecr.0c02494.
URL https://doi.org/10.1021/acs.iecr.0c02494

[30] BASF, AdBlue® Technical Leaflet (November) (2006) 1–6.
URL https://www.gabriels.be/sites/gabriels/files/pdf/technische{_}fiche{_}adblue-{_}engels.pdf

[31] S. Halonen, T. Kangas, M. Haataja, U. Lassi, Urea-Water-Solution Properties: Density, Viscosity, and Surface Tension in an Under-Saturated Solution, Emission Control Science and Technology 3 (2) (2017) 161–170. doi:10.1007/s40825-016-0051-1.